

Claxton Tom (Orcid ID: 0000-0002-8766-3370)
Hossaini Ryan (Orcid ID: 0000-0003-2395-6657)
Wild Oliver (Orcid ID: 0000-0002-6227-7035)
Chipperfield Martyn, P. (Orcid ID: 0000-0002-6803-4149)
Wilson Chris (Orcid ID: 0000-0001-8494-0697)

On the regional and seasonal ozone depletion potential of chlorinated very short-lived substances

Tom Claxton¹, Ryan Hossaini¹, Oliver Wild¹, Martyn P. Chipperfield^{2,3} and Chris Wilson^{2,3}

¹Lancaster Environment Centre, Lancaster University, Lancaster, UK.

²School of Earth and Environment, University of Leeds, Leeds, UK.

³National Centre for Earth Observation, University of Leeds, Leeds, UK.

Corresponding authors: Tom Claxton (t.claxton@lancaster.ac.uk) and Ryan Hossaini (r.hossaini@lancaster.ac.uk)

Key Points:

- Ozone depletion potential of very short-lived substances (CHCl_3 , CH_2Cl_2 , C_2Cl_4 , $\text{C}_2\text{H}_4\text{Cl}_2$) calculated using a 3-D chemical transport model.
- Calculated ozone depletion potentials vary by a factor of 2-3 depending on emission location; larger ODPs for Asian emissions.
- Efficient transport of very short-lived substances from continental East Asia to tropical lower stratosphere leading to larger Asian ODPs.

This article has been accepted for publication and undergone full peer review but has not been through the copyediting, typesetting, pagination and proofreading process which may lead to differences between this version and the Version of Record. Please cite this article as doi: 10.1029/2018GL081455

Abstract

Chloroform (CHCl_3), dichloromethane (CH_2Cl_2), perchloroethylene (C_2Cl_4) and 1,2-dichloroethane ($\text{C}_2\text{H}_4\text{Cl}_2$) are chlorinated Very Short-Lived Substances (Cl-VSLS) with a range of commercial/industrial applications. Recent studies highlight the increasing influence of Cl-VSLS on the stratospheric chlorine budget and therefore their possible role in ozone depletion. Here, we evaluate the ozone depletion potential (ODP) of these Cl-VSLS using a three-dimensional chemical transport model and investigate sensitivity to emission location/season. The seasonal dependence of the ODPs is small but ODPs vary by a factor of 2-3 depending on the continent of emission: 0.0143-0.0264 (CHCl_3), 0.0097-0.0208 (CH_2Cl_2), 0.0057-0.0198 (C_2Cl_4) and 0.0029-0.0119 ($\text{C}_2\text{H}_4\text{Cl}_2$). Asian emissions produce the largest ODPs owing to proximity to the tropics and efficient troposphere-to-stratosphere transport of air originating from industrialised East Asia. The Cl-VSLS ODPs are generally small but the upper ends of the CHCl_3 and CH_2Cl_2 ranges are comparable to the mean ODP of methyl chloride (0.02), a longer-lived ozone-depleting substance.

Plain Language Summary

Anthropogenic emissions of long-lived chlorinated substances (e.g. chlorofluorocarbons, CFCs) has led to global ozone layer depletion since the 1970/80s, including the Antarctic Ozone Hole phenomenon. The 1987 Montreal Protocol was enacted to ban production of major ozone-depleting gases and in consequence there are signs that the ozone layer is recovering. However, emissions of so-called very short-lived substances, such as dichloromethane, have increased in recent years. Historically, these compounds have not been considered a major threat to stratospheric ozone, due to relatively short lifetimes, and they are not controlled by the Protocol. Given that production of these compounds is projected to increase, it is important to determine their ability to affect stratospheric ozone. We quantify the ozone depletion potential (ODP) of chloroform and perchloroethylene, and for the first time, dichloromethane and 1,2-dichloroethane, the main chlorinated very short-lived substances. We show that their ODPs vary depending on where the emission occurs. For example, the ODP from Asian dichloromethane emissions is up to a factor of two greater than that from European emissions. This reflects the relative efficiency of troposphere to stratosphere transport between different geographical areas; the transport of polluted boundary layer air from continental East Asia being one relatively efficient route.

1 Introduction

Chlorinated Very Short-Lived Substances (Cl-VSLS), including chloroform (CHCl_3) and dichloromethane (CH_2Cl_2), are a significant source of stratospheric chlorine [e.g. Laube et al., 2008; Hossaini et al., 2015] and therefore contribute to ozone depletion [e.g. Hossaini et al., 2017; Chipperfield et al., 2018]. These compounds have surface atmospheric lifetimes of ~6 months or less [e.g. Ko et al., 2003] and are used in a variety of commercial and industrial applications. CH_2Cl_2 is a common solvent [e.g. Simmonds et al., 2006], used as a paint stripper and in foam production, among other applications [e.g. Montzka et al., 2011; Feng et al., 2018]. CHCl_3 has historically been used in the production of HCFC-22 and is a by-product of paper manufacturing. Other Cl-VSLS include perchloroethylene (C_2Cl_4), and 1,2-dichloroethane ($\text{C}_2\text{H}_4\text{Cl}_2$), both of which also have significant anthropogenic sources, though shorter atmospheric lifetimes [Montzka et al., 2011].

Owing to increasing emissions, tropospheric CH_2Cl_2 mixing ratios have approximately doubled since the early 2000s, evidenced by long-term surface monitoring data [e.g. Hossaini et al., 2015, 2017] and measurements in the upper troposphere [Leedham Elvidge et al., 2015]. Although the influence of CH_2Cl_2 on ozone has been modest in the recent past [Chipperfield et al., 2018], if sustained CH_2Cl_2 growth continues in coming decades, ozone layer recovery could be delayed [Hossaini et al., 2017]. A substantial portion of CH_2Cl_2 emissions, estimated globally at ~0.8 Tg/yr in 2012 [Carpenter et al., 2014], are believed to occur in Asia [Oram et al., 2017]. CH_2Cl_2 emissions from China, for example, are thought to have increased by a factor of ~3 between 2005 and 2016, with further increases projected until 2030 [Feng et al., 2018].

The ozone depletion potential (ODP) concept [Wuebbles, 1981, 1983, Solomon et al., 1992] was introduced as a relative means to assess a compound's ability to destroy stratospheric ozone. ODP assessment is integral to policy frameworks, notably the Montreal Protocol, which prohibits the production of numerous ozone-depleting substances. For long-lived gases that are well mixed in the troposphere (e.g. CFCs), ODPs are generally independent of emission location and season. However, for VSLS, owing to their short lifetimes, emission location and season have been shown to be important factors [e.g. Ko et al., 2003; Pisso et al., 2010; Brioude et al., 2010]. For particularly short-lived VSLS (e.g. CH_3I , lifetime of days-weeks), the ODP can vary by a factor of ~30 depending on where the emission occurs [Brioude et al., 2010; Harris et al., 2014].

Despite recent interest in Cl-VSLS, very little information on their ODP is present in the literature, and there are no estimates for CH_2Cl_2 and $\text{C}_2\text{H}_4\text{Cl}_2$, to our knowledge. In this study we use a three-dimensional (3-D) chemical transport model (CTM) to quantify the ODP of four Cl-VSLS (CHCl_3 , CH_2Cl_2 , C_2Cl_4 and $\text{C}_2\text{H}_4\text{Cl}_2$). We consider how their ODPs vary with emission location (and season) from five major industrialised geographical areas. Sections 2 and 3 describe the CTM setup and the ODP procedure. Results are presented in Section 4 and conclusions in Section 5. We also calculate the ODP of methyl chloride, a longer-lived chlorocarbon, with a lifetime of ~ 1 year [Montzka et al., 2014].

2 TOMCAT/SLIMCAT 3-D CTM

We performed a series of experiments with the TOMCAT/SLIMCAT 3-D CTM [Chipperfield, 2006; Monks et al., 2017], widely used in VSLS-related studies [e.g. Hossaini et al., 2016a, b]. The CTM is forced by wind and temperature fields from the European Centre for Medium-Range Weather Forecasts (ECMWF) ERA-Interim reanalysis [Dee et al., 2011]. Simulations were performed at a horizontal resolution of $2.8^\circ \times 2.8^\circ$, with 60 vertical levels extending from the surface to ~ 60 km. The CTM exists in both a tropospheric and a stratospheric configuration. In tropospheric mode, convective transport is parameterized based on Tiedtke [1989] and turbulent boundary layer mixing follows Holtslag and Boville [1993]. This model configuration was used to quantify the stratospheric chlorine input due to Cl-VSLS and their product gases, phosgene (COCl_2) and inorganic chlorine (Cl_y). COCl_2 is an oxidation product of CH_2Cl_2 , CHCl_3 , and C_2Cl_4 (**Table S1**), with an assumed tropospheric lifetime of 58 days [Kindler et al., 1995] due to wet deposition.

The stratospheric configuration of TOMCAT/SLIMCAT contains a detailed chemistry scheme covering all major processes relevant to stratospheric ozone loss (e.g. heterogeneous reactions on sulfate aerosols, polar stratospheric clouds etc.). The model version employed here was used by Chipperfield et al. [2018] to investigate long-term ozone trends. Here it is used to determine the response of ozone to stratospheric chlorine perturbations from Cl-VSLS (and products) and to therefore evaluate ODPs. The Cl-VSLS chemistry is consistent between both CTM configurations.

3 ODP calculation

The steady-state ODP (**Equation 1**) of a compound, X, is defined as the global column ozone change due to a unit emission of X, relative to the global column ozone change due to a unit emission of CFC-11 at equilibrium [e.g. Wuebbles et al., 2011]. The ODP of X can therefore

be calculated from a reference stratospheric model run, a model run with X perturbed relative to the reference, and a run with CFC-11 perturbed relative to the reference.

$$\text{ODP}(X) = \frac{\text{Global mean column ozone change due to unit emissions of X}}{\text{Global mean column ozone change due to unit emissions of CFC-11}} \quad \text{Equation 1}$$

The tropospheric TOMCAT/SLIMCAT configuration was first used to calculate the steady-state stratospheric input of CH_2Cl_2 , CHCl_3 , C_2Cl_4 , $\text{C}_2\text{H}_4\text{Cl}_2$ and their products. These steady-state chlorine perturbations were determined using 5 different years of model meteorology (2013-2017) to assess the influence of interannual tropospheric transport variability on our results. As we are principally interested in how chlorine perturbations vary with emission location, a series of tagged Cl-VSLS tracers were emitted from five geographical areas, each at a continuous rate of 1 Tg/yr. The regions (**Figure S1**) are based on the TRANSCOM project [e.g. Gurney et al., 2003] and broadly correspond to major industrialized areas: Temperate North America (TemNA), Europe (Eur), Temperate Latin America (TemLA), Temperate Asia (TemAs) and Tropical Asia (TroAs). A 1 Tg/yr emission was chosen as it is similar to current global estimates of CH_2Cl_2 emissions [Hossaini et al., 2017].

Within regions, the Cl-VSLS emission distribution followed the industrial scenario [McCulloch et al., 1999; Keene et al., 1999] of the Reactive Chlorine Emissions Inventory (RCEI). For $\text{C}_2\text{H}_4\text{Cl}_2$, not considered by the RCEI, the same distribution as CH_2Cl_2 was assumed – reasonable given their observed correlation [Oram et al., 2017]. Although the RCEI was undertaken over 20 years ago, the broadscale industrial emission distribution within our regions is unlikely to have changed to such a degree to significantly affect our results. This is particularly true of Europe and North America, though Asian regions may have seen larger changes to the distribution. To test the influence of emission distributions, we also considered Cl-VSLS tracers emitted with uniformly distributed fluxes within each region; i.e. an extreme departure from the RCEI case.

Species	Emission region	Annual mean stratospheric Cl perturbation (ppt Cl)		Seasonal mean (RCEI distr.) stratospheric Cl perturbation (ppt Cl)				SGI % (RCEI distr.)
		<i>Evenly distributed emission</i>	<i>RCEI distributed emissions</i>	<i>DJF</i>	<i>MAM</i>	<i>JJA</i>	<i>SON</i>	
CHCl ₃	Eur	79.2 ± 1.0	79.1 ± 1.0	73.6 ± 0.7	75.2 ± 2.2	82.7 ± 1.5	84.9 ± 0.9	61.6
	TemAs	97.6 ± 2.1	99.5 ± 2.0	93.7 ± 1.7	89.8 ± 2.9	102.1 ± 2.7	112.4 ± 3.4	65.3
	TemLA	79.1 ± 0.6	78.7 ± 0.6	82.0 ± 0.8	84.2 ± 0.9	74.5 ± 1.0	74.0 ± 1.2	60.8
	TemNA	84.1 ± 0.9	82.0 ± 0.8	77.4 ± 0.7	78.6 ± 1.8	85.1 ± 1.2	86.9 ± 1.1	61.9
	TroAs	130.5 ± 5.5	120.0 ± 4.8	118.9 ± 4.5	113.3 ± 7.3	120.3 ± 5.7	127.3 ± 6.4	68.4
CH ₂ Cl ₂	Eur	59.1 ± 0.9	55.8 ± 0.8	51.2 ± 0.7	54.3 ± 1.8	59.4 ± 1.0	58.3 ± 0.7	76.5
	TemAs	75.3 ± 1.7	71.0 ± 1.3	67.8 ± 0.8	66.4 ± 2.2	72.5 ± 1.5	77.2 ± 2.2	77.6
	TemLA	59.6 ± 0.5	58.9 ± 0.5	60.9 ± 0.7	62.6 ± 1.1	56.0 ± 0.8	56.1 ± 1.1	75.1
	TemNA	63.3 ± 0.8	61.8 ± 0.8	57.8 ± 1.0	60.6 ± 1.8	65.0 ± 0.8	63.6 ± 1.2	76.6
	TroAs	105.5 ± 4.9	99.3 ± 4.8	99.9 ± 4.5	95.0 ± 7.3	99.4 ± 5.9	102.8 ± 6.2	80.0
C ₂ Cl ₄	Eur	24.0 ± 0.5	22.6 ± 0.5	20.7 ± 0.5	22.4 ± 1.2	23.9 ± 0.6	23.4 ± 0.4	38.2
	TemAs	37.7 ± 1.5	34.3 ± 1.1	32.8 ± 0.7	30.4 ± 1.6	34.3 ± 1.3	39.7 ± 2.1	42.5
	TemLA	25.5 ± 0.4	24.8 ± 0.4	25.7 ± 0.6	27.2 ± 0.9	22.9 ± 0.5	23.4 ± 0.8	38.5
	TemNA	27.1 ± 0.6	25.9 ± 0.6	24.7	25.8 ± 0.9	26.7	26.3	39.3

	TroAs	66.1 ± 4.6	60.7 ± 4.6	± 0.9	1.4	± 0.4	± 0.8	48.1
				± 4.1	6.7	± 5.7	± 6.0	
C ₂ H ₄ Cl ₂	Eur	16.8 ± 0.5	15.7 ± 0.4	13.8	17.0 ± 1.1	17.5	14.4	75.7
				± 0.6	1.1	± 0.4	± 0.4	
	TemAs	27.1 ± 1.1	24.0 ± 0.8	23.0	22.5 ± 1.4	24.1	26.4	76.8
				± 0.5	1.4	± 0.8	± 1.6	
	TemLA	16.5 ± 0.3	15.8 ± 0.4	16.1	17.0 ± 0.7	14.8	15.2	75.7
				± 0.5	0.7	± 0.4	± 0.7	
	TemNA	18.8 ± 0.5	17.8 ± 0.5	16.5	19.2 ± 1.2	19.2	16.5	76.1
				± 0.8	1.2	± 0.3	± 0.7	
	TroAs	49.8 ± 3.9	44.9 ± 3.7	46.5	41.7 ± 5.4	43.9	47.7	78.5
				± 3.4	5.4	± 4.5	± 5.0	

Table 1. Modelled stratospheric Cl perturbations (ppt Cl) due to a 1 Tg/yr VLSL emission from different regions. Steady-state perturbations derived as sum of chlorine from source and product gases at the tropical ($\pm 20^\circ$ latitude) tropopause (16.5-17.5 km). Perturbations are annual 5-year means (2013-2017 meteorology, $\pm 1\sigma$) and are presented for the evenly-distributed and the RCEI-distributed emissions. Seasonal values (5-year mean $\pm 1\sigma$) assume RCEI distribution. Final column gives annual total Cl perturbation due to source gas injection (SGI, %).

The above approach was also used to calculate the steady-state CFC-11 stratospheric perturbation following a continuous 50 Gg/yr surface emission. This moderate emission rate was chosen to (a) avoid any possible non-linearities in the ozone response for large chlorine perturbations and (b) give a response above the model's numerical noise [e.g. Wuebbles et al., 1998]. The resulting stratospheric CFC-11 perturbation (~ 100 ppt) produces a global mean column ozone decrease of $\sim 1\%$, consistent with previous work [Wuebbles et al., 1998]. The calculated range (due to different emission locations/distribution) of stratospheric Cl-VLSL perturbations (and the CFC-11 perturbation) were used as input to the detailed stratospheric chemistry model (Section 2). For each chlorine perturbation, the ozone response was calculated relative to a reference unperturbed stratosphere, allowing ODPs to be quantified from Equation 1.

4.1 Hemispheric and Zonal Source Gas Distributions

A key consideration is whether anthropogenic emissions from Northern Hemisphere (NH) mid-latitudes and sub-tropics (including major Asian economies) can sustain significant Cl-VSLS mixing ratios in the tropics, where troposphere-to-stratosphere transport takes place. **Figure 1** compares the modelled CH_2Cl_2 abundance at the surface and at 90 hPa (~ 17 km, location of tropical tropopause), resulting from a 1 Tg/yr emission from four of the five regions considered. Note, Temperate North America, not shown for clarity, shows a similar hemispheric distribution to Europe. Similar figures for other Cl-VSLS are given in **Figures S2-S4**.

Emissions from mid-latitude and sub-tropical regions establish a strong CH_2Cl_2 hemispheric gradient at the surface (**Figure 1**, left column). Zonally, surface CH_2Cl_2 is relatively well mixed away from main industrialised areas where clear maxima occur. The tropical ($\pm 20^\circ$) 5-year mean surface CH_2Cl_2 mixing ratios at steady state are 29 ppt (emission from TemNA), 26 ppt (Eur), 30 ppt (TemAs), 39 ppt (TroAs) and 37 ppt (TemLA). Proximity to the tropics is clearly a large influence on these values, with TroAs emissions sustaining the largest tropical CH_2Cl_2 levels. The spread in these values is $\sim 40\%$, with Eur and TemNA emissions resulting in similar tropical surface CH_2Cl_2 abundances that are a factor of 1.5 lower than that resulting from TroAs emissions. While transport of Cl-VSLS to the stratosphere will be relatively inefficient over these regions, the CH_2Cl_2 lifetime is sufficiently long to allow meridional transport to sustain non-negligible CH_2Cl_2 abundances in the tropical boundary layer (e.g. **Figure 1a**). Once in the tropical troposphere, vertical gradients in zonally averaged CH_2Cl_2 are generally small [Hossaini et al., 2016b; also **Figure 2**].

Tropical CH_2Cl_2 is reasonably well mixed at 90 hPa, the approximate tropical tropopause. Compared to analogous brominated compounds such as CHBr_3 (24-day lifetime in tropical boundary layer) and CH_2Br_2 (94 days), Cl-VSLS are relatively long-lived, thus sub-grid scale transport processes (e.g. convection) are a less important influence for their troposphere-to-stratosphere transport. For CHBr_3 , for example, previous model studies highlighted strong zonal variability in its tropical near-tropopause abundance [e.g. Aschmann et al., 2011; Hossaini et al., 2016a]. The largest levels have been predicted in strong convective regions, including the Indian Ocean, Central America and the Maritime Continent [e.g. Gettelman et al., 2009; Hosking et al., 2010; Aschmann et al., 2011; Liang et al., 2014]. Such strong zonal

variability is less apparent for CH_2Cl_2 apart from in the case of Asia emissions (particularly tropical) which co-located with such transport processes (**Figure 1h**).

4.2 Stratospheric Chlorine Perturbations

A summary of modelled stratospheric Cl perturbations from Cl-VSLS is given in **Table 1**. These steady-state perturbations are calculated as the sum of chlorine in both source and product gases, expressed as annual/seasonal means over a 5-year period, 2013-2017. Due to the latter, these values are more representative than considering a single year of meteorology. Regardless of emission location, the Cl perturbation is greatest for CHCl_3 (91.9 ppt Cl), followed by CH_2Cl_2 (69.4 ppt Cl), C_2Cl_4 (33.7 ppt Cl) and $\text{C}_2\text{H}_4\text{Cl}_2$ (23.6 ppt Cl). Recall, these perturbations are based on a 1 Tg/yr source gas emission, with the values quoted above being all-region averages, assuming the RCEI emission distribution. For a given region, differing Cl perturbations across species reflects the different chlorine atomicity and tropospheric lifetimes of the compounds. In the tropical boundary layer, local lifetimes of CHCl_3 , CH_2Cl_2 , C_2Cl_4 and $\text{C}_2\text{H}_4\text{Cl}_2$ were assessed to be 112, 109, 67, and 47 days, respectively [Carpenter et al., 2014], consistent with the relative importance of each compound described above and in good agreement to our model estimates (**Table S2**).

Table 1 reveals that differences between tracers with the RCEI emission distribution and those evenly-distributed is small; e.g. the all-region mean Cl perturbation from CH_2Cl_2 is 69.4 ppt Cl (RCEI) and 72.6 ppt Cl (even), agreeing to within 4.6%. We focus herein on the RCEI case, noting that small differences between the scenarios is likely caused by how close the emissions are distributed to the tropics, where troposphere-to-stratosphere transport takes place. Indeed, for this reason, calculated Cl perturbations exhibit significant sensitivity to the continental scale location of emission, consistent with the known dependence of VSLS emission location on their ODPs [e.g. Bridgeman et al., 2000; Brioude et al., 2010]. The spread in stratospheric Cl perturbations due to emission location is 52% (CHCl_3), 78% (CH_2Cl_2), 169% (C_2Cl_4) and 186% ($\text{C}_2\text{H}_4\text{Cl}_2$), with longer-lived compounds exhibiting a lower sensitivity. The seasonal dependence of stratospheric Cl perturbations is far smaller. For example, for a given region of CH_2Cl_2 emission, the seasonal spread is ~10% or less. Therefore, we do not overinterpret our findings in terms of seasonality, though note that seasonal differences reflect the complex interaction of (a) seasonality in transit times for NH air reaching the tropics [Orbe et al., 2016], low level flow into areas of convection [Pisso et

al., 2010], seasonality in vertical transport efficiency through the tropical tropopause layer [e.g., Krüger et al., 2009; Hosking et al., 2010; Bergman et al., 2012], and interaction of such processes with region-dependent Cl-VSLs lifetimes [Brioude et al., 2010].

Tropical Asia emissions lead to the largest stratospheric Cl injections, coinciding with efficient troposphere-to-stratosphere transport over the Maritime Continent [e.g. Hosking et al., 2010; Wright et al., 2011]. Temperate Asia is the second most efficient region, most likely due to its locality towards tropical Asia and reflecting the efficient transport of polluted airmasses originating from continental East Asia to the deep tropics and tropical upper troposphere [Orbe et al., 2015; Ashfold et al., 2015; Oram et al., 2017]. Note, our stratospheric chlorine perturbations are somewhat, but not strongly, influenced by the year of meteorology under consideration, as evident by the $\pm 1\sigma$ values in **Table 1**. These standard deviations (σ) are calculated on the 5-year mean Cl perturbations and in relative terms (the ratio of σ to the mean) range from 0.8-8%. The two Asian regions are impacted the largest by interannual variability, indicating that transport processes have greater leverage to influence VSLs troposphere-to-stratosphere transport from these regions compared to others.

4.3 Source Gas versus Product Gas Injection

Table 1 also shows the percentage of total chlorine that enters the stratosphere via source gas injection (SGI). For a given species, the regional spread in these values is generally small, with emissions from tropical Asia resulting in the largest SGI components. CH_2Cl_2 has the largest proportion of SGI (75-80%) and C_2Cl_4 (38-48%) the least. The relative importance of SGI versus Product Gas Injection (PGI) depends on both the lifetime of the source gases and the different combination of product gases (COCl_2 and Cl_y) produced. **Figure 2** shows vertically-resolved tropical mean profiles of the contribution of SGI versus PGI, using European emissions as an example.

In terms of the total tropospheric chlorine budget arising from CHCl_3 and CH_2Cl_2 , source gases are the most important component (accounting for ~60-80% at the tropical tropopause, **Table 1**), followed by phosgene. CHCl_3 and CH_2Cl_2 have similar lifetimes and the larger phosgene component in the budget of the former reflects the larger phosgene yield from the $\text{CHCl}_3 + \text{OH}$ sink, compared to that from CH_2Cl_2 oxidation (**Text S1**). For C_2Cl_4 , delivery of chlorine to the stratosphere via SGI and PGI are comparable, with the latter slightly larger. This reflects the shorter C_2Cl_4 lifetime compared to CHCl_3 and CH_2Cl_2 and the significant phosgene yield from C_2Cl_4 oxidation. Note, a source of uncertainty (see also Section 4.4) in

our model is the assumed tropospheric washout lifetimes of phosgene and Cl_y products (Text S1). This uncertainty is more relevant to the two shortest-lived compounds under consideration (C_2Cl_4 and $\text{C}_2\text{H}_4\text{Cl}_2$).

4.4 ODP Calculations

The stratospheric chlorine injections discussed in Section 4.2 were added as tropopause boundary conditions in the stratospheric TOMCAT/SLICMAT model configuration. For each Cl-VSLS, three stratospheric simulations were performed, the first with the mean Cl perturbation from the five (RCEI-distributed) regions (**Table 1**). The second and third experiments were designed to represent the lower and upper bounds of the Cl perturbations, incorporating the regional/seasonal spread. Thus, the mean Cl perturbations were multiplied by 0.5 and 1.5 to approximate the lower and upper bounds, respectively (**Table S3**). Each perturbation experiment was run for 25 years to allow a new ozone steady state to be established with respect to the reference run (**Figure S5**).

There is a strong linearity ($|R| > 0.999$) between stratospheric Cl from Cl-VSLS and the resulting global mean column ozone change (Dobson Units, DU), see **Figure S6**. For each Cl-VSLS considered, the linear ozone responses allow the ozone change due to any chlorine perturbations in **Table 1** to be calculated. Note that the global average loss of ozone due to the CFC-11 perturbation was -3.8 DU, based on a 50 Gg/yr surface emission. As the ozone responses are proportional to the emissions, the corresponding ozone change for a 1 Tg/yr CFC-11 emission is readily calculated, allowing ODPs to be derived using **Equation 1**. An example latitude-height cross section of ozone changes due to VSLS and due to CFC-11 is given in **Figure S7**. Chlorine derived from either compound depletes ozone in the same regions, that is where ozone loss cycles involving chlorine are efficient; i.e. notably the polar lower stratosphere and upper stratosphere.

Figure 3 shows the range of ODPs for each Cl-VSLS grouped by emission location and season (see also **Table S4**). Our results are in qualitative agreement with previous studies, highlighting an emission location- and seasonal-dependence of VSLS ODPs in general [e.g. Pisso et al., 2010; Brioude et al., 2010]. However, as those previous studies have largely focussed on particularly short-lived VSLS, it is notable that the spread in derived ODPs for Cl-VSLS assessed here is generally smaller, particularly for seasonal variations. For example, Pisso et al [2010] showed that the ODP of n-propyl bromide (~20-day lifetime), when emitted from NH mid-latitudes (30°N-60°N), varied by a factor of ~2.5 between NH summer

and winter. In contrast, the seasonal spread in Cl-VSLS here is far smaller, and a factor of ~ 2.5 is more similar to the *total* ODP spread taking into account the larger variability introduced by emission location.

Few ODP estimates for Cl-VSLS are available in the literature. For CHCl_3 and C_2Cl_4 , Kindler et al. [1995] reported values of ~ 0.01 and ~ 0.006 , respectively. Our CHCl_3 ODP range (0.0143-0.0264) is larger than these semi-empirical Kindler et al. [1995] estimates, though our C_2Cl_4 range (0.0057-0.0198) incorporates their estimate at the lower limit. Our lower ODP limit for C_2Cl_4 is also 14% larger than the 0.005 reported by a previous 3-D model study [Wuebbles et al., 2011]. However, that work assumed that all chlorine released from tropospheric C_2Cl_4 oxidation was in the form of Cl_y , which is subject to deposition. Our study also considered phosgene as an intermediate, which is expected to have a longer tropospheric lifetime versus deposition [Kindler et al., 1995] and is thus a relatively efficient carrier of chlorine to the stratosphere.

Our derived ODP range for CH_2Cl_2 is 0.0097-0.0208 and to the best of our knowledge this is the first estimate for this compound. The range is skewed by the larger values from the Asian emission scenarios, particularly tropical Asia, as is the case for each Cl-VSLS considered. For example, CH_2Cl_2 ODPs are a factor of two larger when emissions are concentrated in tropical Asia as opposed to Europe, with emissions from the latter resulting in the lowest ODPs. The CH_2Cl_2 ODPs from the temperate Asia emission scenario (**Figure 3**) are also larger with respect to the all-region all-season mean (**Table S4**); significant as (a) efficient troposphere-to-stratosphere transport routes exist for emissions from this region [Ashfold et al. 2015; Oram et al., 2017; **Figure 1**] and (b) regional CH_2Cl_2 emissions are expected to further increase in coming years [Feng et al., 2018]. The derived ODPs for $\text{C}_2\text{H}_4\text{Cl}_2$ are in the range 0.0029-0.0119 and are the lowest of the species considered.

Our study shows Cl-VSLS have generally small ODPs. For context, the ODP of some major substances controlled by the Montreal Protocol [Harris et al., 2014] are 1.0 (CFC-11), 0.73 (CFC-12), and 0.81 (CFC-113). We also calculated the ODP of methyl chloride (CH_3Cl) using the same experimental setup as for Cl-VSLS (**Table S4**). The CH_3Cl ODP range is 0.0188-0.0262, with an average ODP of 0.02. This is in good agreement with previous estimates of ~ 0.02 [Harris and Wuebbles et al., 2014] and shows that, at the upper limit, CHCl_3 and CH_2Cl_2 have comparable ODPs to CH_3Cl despite their shorter atmospheric lifetimes (reflecting the multiple Cl atoms of these Cl-VSLS). It is important to note that

product gases account for a significant portion of the chlorine injected into the stratosphere from VSLS (**Table 1**). As details of product chemistry are uncertain, we also quantified ODPs under the assumption that no product gases reach the stratosphere. Naturally, these ODPs are smaller and represent lower limits (**Table S4**). Finally, while ODPs for Cl-VSLS are not strongly influenced by interannual variability in our model, details of tropospheric transport can vary greatly between models, including those running with the same reanalysis meteorology [Orbe et al., 2016]. On this basis, we recommend other modelling groups quantify VSLS ODPs to corroborate our findings.

5 Concluding Remarks

A 3-D CTM was used to quantify the ODP of CHCl_3 , CH_2Cl_2 , C_2Cl_4 and $\text{C}_2\text{H}_4\text{Cl}_2$, and to investigate sensitivity to emissions location and season. Determining the ability of these compounds to influence stratospheric ozone is important given recently reported increases in CH_2Cl_2 emissions and projections of further increases [Feng et al., 2018]. The derived ODP ranges reveal a small but significant potential for Cl-VSLS to influence ozone, particularly if emissions are located in close proximity to the tropics: CHCl_3 (0.0143-0.0264), CH_2Cl_2 (0.0098-0.0208), C_2Cl_4 (0.0057-0.0198) and $\text{C}_2\text{H}_4\text{Cl}_2$ (0.0029-0.0119). Our simulations indicate (a) relatively efficient transport of Cl-VSLS originating from continental east Asia to the lower stratosphere, in support of recently proposed transport pathways, and (b) that VSLS emissions resulting from the industrialization of South East Asia have up to a factor of 3 times greater potential to influence stratospheric ozone than emissions from Europe.

Acknowledgements

This work was supported by RH's NERC Fellowship (NE/N014375/1) and the SISLAC project (NE/R001782/1). MPC is supported by a Wolfson Merit Award. We thank Wuhu Feng for TOMCAT/SLIMCAT model development. Model data is available at the Lancaster University data repository (doi:10.17635/lancaster/researchdata/283). The Supporting Information consists of 7 figures and 4 tables.

References

- Aschmann, J., Sinnhuber, B.-M., Chipperfield, M. P., & Hossaini, R. (2011). Impact of deep convection and dehydration on bromine loading in the upper troposphere and lower stratosphere, *Atmospheric Chemistry and Physics*, **11**, 2671-2687.
<https://doi.org/10.5194/acp-11-2671-2011>.
- Ashfold, M. J., Pyle, J. A., Robinson, A. D., Meneguz, E., Nadzir, M. S. M., Phang, S. M., et al. (2015). Rapid transport of East Asian pollution to the deep tropics. *Atmospheric Chemistry and Physics*, **15**(6), 3565–3573. doi:10.5194/acp-15-3565-2015.
- Bergman, J. W., Jensen, E. J., Pfister, L., & Yang, Q. (2012). Seasonal differences of vertical-transport efficiency in the tropical tropopause layer: On the interplay between tropical deep convection, large-scale vertical ascent, and horizontal circulations, *Journal of Geophysical Research*, **117**(D5), D05302. doi: 10.1029/2011JD016992.
- Bridgeman, C. H., Pyle, J. A., & Shallcross, D. E. (2000). A three-dimensional model calculation of the ozone depletion potential of 1-bromopropane (1-C₃H₇Br), *Journal of Geophysical Research*, **105**, 26493–26502. <https://doi.org/10.1029/2000JD900293>.
- Brioude, J., Portmann, R. W., Daniel, J. S., Cooper, O. R., Frost, G. J., Rosenlof, K. H., et al. (2010). Variations in ozone depletion potentials of very short-lived substances with season and emission region, *Geophysical Research Letters*, **37**, L19804.
<https://doi.org/10.1029/2010GL044856>.
- Burkholder, J. B., Sander, S. P., Abbatt, J., Barker, J. R., Huie, R. E., Kolb, C. E., et al. (2015). Chemical kinetics and photochemical data for use in atmospheric studies, Evaluation number 18, *JPL Publication 15-10*, Jet Propulsion Laboratory, Pasadena.
<http://jpldataeval.jpl.nasa.gov/>
- Carpenter, L. J., Reiman, S., Burkholder, J. B., Clerbaux, C., Hall, B. D., Hossaini, R., et al. (2014). Ozone-depleting substances (ODSs) and other gases of interest to the Montreal Protocol. In Engel, A., & Montzka, S.A., *Scientific assessment of ozone depletion: 2014, global ozone research and monitoring project-Report No. 55*, World Meteorological Organization, Geneva, Switzerland.

Chipperfield, M. P. (2006). New version of the TOMCAT/SLIMCAT off-line chemical transport model: Intercomparison of stratospheric tracer experiments, *Quarterly Journal of the Royal Meteorological Society*, **132**(617), 1179–1203. <http://doi.org/10.1256/qj.05.51>.

Chipperfield, M. P., Dhomse, S., Hossaini, R., Feng, W., Santee, M. L., Weber, M., et al. (2018). On the cause of recent variations in lower stratospheric ozone, *Geophysical Research Letters*, **45**, 5718-5726. <https://doi.org/10.1029/2018GL078071>.

Dee, D., Uppala, S., Simmons, A., Berrisford, P., Poli, P., Kobayashi, S., et al. (2011). The ERA-Interim reanalysis: Configuration and performance of the data assimilation system, *Quarterly Journal of the Royal Meteorological Society*, **137**(656), 553–597. <https://doi.org/10.1002/qj.828>.

Feng, Y., Bie, P., Wang, Z., Wang, L., & Zhang, J., (2018). Bottom-up anthropogenic dichloromethane emission estimates from China for the period 2005–2016 and predictions of future emissions, *Atmospheric Environment*, **186**, 241-247. <https://doi.org/10.1016/j.atmosenv.2018.05.039>.

Gettelman, A., Lauritzen, P. H., Park, M., & Kay, J. E. (2009). Processes regulating short-lived species in the tropical tropopause layer, *Journal of Geophysical Research*, **114**, D13303. doi: 10.1029/2009JD011785.

Gurney, K. R., Law, R. M., Denning, A. S., Rayner, P. J., Baker, D., Bousquet, P., et al. (2003). Transcom 3 CO₂ Inversion Intercomparison: 1. Annual mean control results and sensitivity to transport and prior flux information, *Tellus Series B: Chemical and Physical Meteorology*, **55**, 555-579. DOI:10.1034/j.1600-0889.2003.00049.x

Harris, N. R. P., Wuebbles, D. J., Daniel, J. S., Hu, J., Kuijpers, L. J. M., et al. (2014). Scenarios and information for policymakers. In Engel, A. & Montzka, S.A., *Scientific assessment of ozone depletion: 2014, global ozone research and monitoring project-Report No. 55*, World Meteorological Organization, Geneva, Switzerland.

Holtslag, A., & Boville, B. (1993): Local versus nonlocal boundary-layer diffusion in a global climate model, *Journal of Climate*, **6**, 1825–1842. [https://doi.org/10.1175/1520-0442\(1993\)006<1825:LVNBLD>2.0.CO;2](https://doi.org/10.1175/1520-0442(1993)006<1825:LVNBLD>2.0.CO;2).

Hosking, J. S., Russo, M. R., Braesicke, P., & Pyle, J. A. (2010). Modelling deep convection and its impacts on the tropical tropopause layer, *Atmospheric Chemistry and Physics*, **10**(22), 11175–11188. doi: 10.5194/acp-10-11175-2010.

Hossaini, R., Chipperfield, M. P., Saiz-Lopez, A., Harrison, J. J., von Glasow, R., Sommariva, R., et al. (2015).: Growth in stratospheric chlorine from short-lived chemicals not controlled by the Montreal Protocol, *Geophysical Research Letters*, **42**, 4573–4580. doi:10.1002/2015GL063783.

Hossaini, R., Patra, P. K., Leeson, A. A., Kryzstofiak, G., Abraham, N. L., Andrews, S. J., et al. (2016a). A multi-model intercomparison of halogenated very short-lived substances (TransCom-VSLS): Linking oceanic emissions and tropospheric transport for a reconciled estimate of the stratospheric source gas injection of bromine, *Atmospheric Chemistry Physics*, **16**, 9163–9187. <https://doi.org/10.5194/acp-16-9163-2016a>.

Hossaini, R., Chipperfield, M. P., Saiz-Lopez, A., Fernandez, R., Monks, S., Feng, W., et al. (2016b). A global model of tropospheric chlorine chemistry: Organic versus inorganic sources and impact on methane oxidation, *Journal of Geophysical Research: Atmospheres*, **121**, 14,271–14,297. doi:10.1002/2016JD025756.

Hossaini, R., Chipperfield, M. P., Montzka, S. A., Leeson, A. A., Dhomse, S. S., & Pyle, J. A. (2017). The increasing threat to stratospheric ozone from dichloromethane, *Nature Communications*, **8**, 1-9. <https://doi.org/10.1038/ncomms15962>.

Keene, W. C., Khalil, M. A. K., Erickson III, D. J., McCulloch, A., Graedel, T. E., Lobert, J. M., et al. (1999). Composite global emissions of reactive chlorine from anthropogenic and natural sources: Reactive chlorine emissions inventory, *Journal of Geophysical Research*, **104**, 8429–8440. <https://doi.org/10.1029/1998JD100084>.

Kindler, T. P., Chameides, W. L., Wine, P. H., Cunnold, D. M., Alyea, F. N., & Franklin, J. A. (1995). The fate of atmospheric phosgene and the stratospheric chlorine loadings of its parent compounds: CCl₄, C₂Cl₄, C₂Cl₃, CH₃CHCl₃, and CHCl₃, *Journal of Geophysical Research*, **100**, 1235–1251. <https://doi.org/10.1029/94JD02518>.

Ko, M. K. W., Poulet, G., Blake, D. R., Boucher, O., Burkholder, J. H., Chin, M., et al. (2003). Very short-lived halogen and sulfur substances. In *Scientific assessment of ozone depletion: 2002, global ozone research and monitoring project—Report No. 47*, World Meteorological Organization, Geneva, Switzerland.

Laube, J. C., Engel, A., Bönisch, H., Möbius, T., Worton, D. R., Sturges, W. T., et al. (2008). Contribution of very short-lived organic substances to stratospheric chlorine and bromine in the tropics – a case study, *Atmospheric Chemistry and Physics*, **8**, 7325–7334. doi:10.5194/acp-8-7325-2008.

Leedham Elvidge, E. C., Oram, D. E., Laube, J. C., Baker, A. K., Montzka, S. A., Humphrey, S., O'Sullivan, D. A., & Brenninkmeijer, C. A. M. (2015). Increasing concentrations of dichloromethane, CH₂Cl₂, inferred from CARIBIC air samples collected 1998-2012, *Atmospheric Chemistry and Physics*, **15**, 1939-1958. <https://doi.org/10.5194/acp-15-1939-2015>.

Liang, Q., Atlas, E., Blake, D., Dorf, M., Pfeilsticker, K., & Schauffler, S. (2014). Convective transport of very short lived bromocarbons to the stratosphere, *Atmospheric Chemistry and Physics*, **14**, 5781–5792. doi:10.5194/acp-14-5781-2014.

McCulloch, A. Aucott, M. L., Benkovitz, C. M., Graedel, T. E., Kleiman, G., & Midgley, M. (1999). Global emissions of hydrogen chloride and chloromethane from coal combustion, incineration and industrial activities: reactive chlorine emissions inventory, *Journal of Geophysical Research*, **104**, 8391-8403. doi:10.1029/1999JD900025.

Monks, S. A., Arnold, S. R., Hollaway, M. J., Pope, R. J., Wilson, C., Feng, W., et al. (2017). The TOMCAT global chemical transport model v1.6: description of chemical mechanism and model evaluation, *Geoscientific Model Development*, **10**, 3015-3057. <https://doi.org/10.5194/gmd-10-3025-2017>.

Montzka, S. A., Reimann, S., Engel, A., Kruger, K., O'Doherty, S., Sturges, W. T., et al., (2011). Ozone-depleting substances (ODSs) and related chemicals. In *Scientific assessment of ozone depletion: 2010, global ozone research and monitoring project-Report No. 52*, World Meteorological Organization, Geneva, Switzerland.

Oram, D. E., Ashfold, M. J., Laube, J. C., Gooch, L. J., Humphrey, S., Sturges, W. T., et al. (2017). A growing threat to the ozone layer from short-lived anthropogenic chlorocarbons, *Atmospheric Chemistry and Physics*, **17**(19), 11,929–11,941. <https://doi.org/10.5194/acp-17-11929-2017>.

Orbe, C., Waugh, D. W., & Newman, P. A., (2015). Air-mass origin in the tropical lower stratosphere: The influence of Asian boundary layer air, *Geophysical Research Letters*, **42** (10): 4240-4248. doi:10.1002/2015gl063937.

Orbe, C., Waugh, D. W., Newman, P. A., & Steenrod, S., (2016). The transit-time distribution from the Northern Hemisphere midlatitude surface, *Journal of Atmospheric Science*, **73**, 10, 3785-3802, doi:10.1175/JAS-D-15-0289.1.

Patra, P. K., Houweling, S., Krol, M., Bousquet, P., Belikov, D., Bergmann, D., et al. (2011). TransCom model simulations of CH₄ and related species: linking transport, surface flux and chemical loss with CH₄ variability in the troposphere and lower stratosphere, *Atmospheric Chemistry and Physics*, **11**, 12813-12837, <https://doi.org/10.5194/acp-11-12813-2011>.

Pisso, I., Haynes, P. H., & Law, K. S. (2010). Emission location dependent ozone depletion potentials for very short-lived halogenated species, *Atmospheric Chemistry and Physics*, **10**, 12025–12036. doi:10.5194/acp-10-12025-2010.

Sherwen, T., Schmidt, J. A., Evans, M. J., Carpenter, L. J., Großmann, K., Eastham, S. D., et al. (2016). Global impacts of tropospheric halogens (Cl, Br, I) on oxidants and composition in GEOS-Chem, *Atmospheric Chemistry and Physics*, **16**, 12239-12271. <https://doi.org/10.5194/acp-16-12239-2016>.

Simmonds, P. G., Manning, A. J., Cunnold, D. M., McCulloch, A., O'Doherty, S., Derwent, R. G., et al., (2006). Global trends, seasonal cycles, and European emissions of dichloromethane, trichloroethene, and tetrachloroethene from the AGAGE observations at Mace Head, Ireland, and Cape Grim, Tasmania, *Journal of Geophysical Research*, **111**, D18304, doi:10.1029/2006JD007082.

Solomon, S., & Albritton, D. L. (1992). A new analysis of time-dependent ozone depletion potentials, *Nature*, **357**, 33–37, 1992.

Tiedtke, M. (1989). A comprehensive mass flux scheme for cumulus parameterization in large-scale models, *Monthly Weather Review*, **117**, 1779–1800. doi:10.1175/1520-0493(1989)117<1779:ACMFSF>2.0.CO;2.

Tuazon, E. C., Atkinson, R., Aschmann, S. M., Goodman, M. A. & Winer, A. M. (1988). Atmospheric reactions of chloroethenes with the OH radical, *International Journal of Chemical Kinetics*, **20**, 241-265. <https://doi.org/10.1002/kin.550200305>.

Wallington, T. J., Bilde, M., Møgelberg, T. E., Sehested, J., & Nielsen, O. J. (1996). Atmospheric Chemistry of 1,2-Dichloroethane: UV Spectra of CH₂ClCHCl and CH₂ClCHClO₂ Radicals, Kinetics of the Reactions of CH₂ClCHCl Radicals with O₂ and

CH₂ClCHClO₂ Radicals with NO and NO₂, and Fate of the Alkoxy Radical CH₂ClCHClO, *Journal of Physical Chemistry*, **100**(14), 5751–5760, doi:10.1021/jp952149g.

Wright, J. S., Fu, R., Fueglistaler, S., Liu, Y. S., & Zhang, Y. (2011). The influence of summertime convection over Southeast Asia on water vapor in the tropical stratosphere, *Journal of Geophysical Research*, **116**(D12), D12302, doi:10.1029/2010JD015416, 2011.

Wuebbles, D. J. (1981). The relative efficiency of a number of halocarbons for destroying stratospheric ozone, (Report UCID-1824). Lawrence Livermore National Laboratory.

Wuebbles, D. J. (1983). Chlorocarbon emission scenarios: potential impact on stratospheric ozone. *Journal of Geophysical Research*, **88**, 1433-1443.

Wuebbles, D. J., Jain, A. K., Patten, K. O., & Connell, P. S. (1998). Evaluation of ozone depletion potentials for chlorobromomethane (CH₂ClBr) and 1-bromo propane (C₃H₇Br), *Atmospheric Environment*, **32**, 107-114. [https://doi.org/10.1016/S1352-2310\(97\)00322-1](https://doi.org/10.1016/S1352-2310(97)00322-1).

Wuebbles, D. J., Patten, K. O., Wang, D., Youn, D., Martínez-Avilés, M., & Francisco, J. S., (2011). Three-dimensional model evaluation of the ozone depletion potentials for n-propyl bromide, trichloroethylene and perchloroethylene, *Atmospheric Chemistry and Physics*, **11**, 2371-2380, <https://doi.org/10.5194/acp-11-2371-2011>.

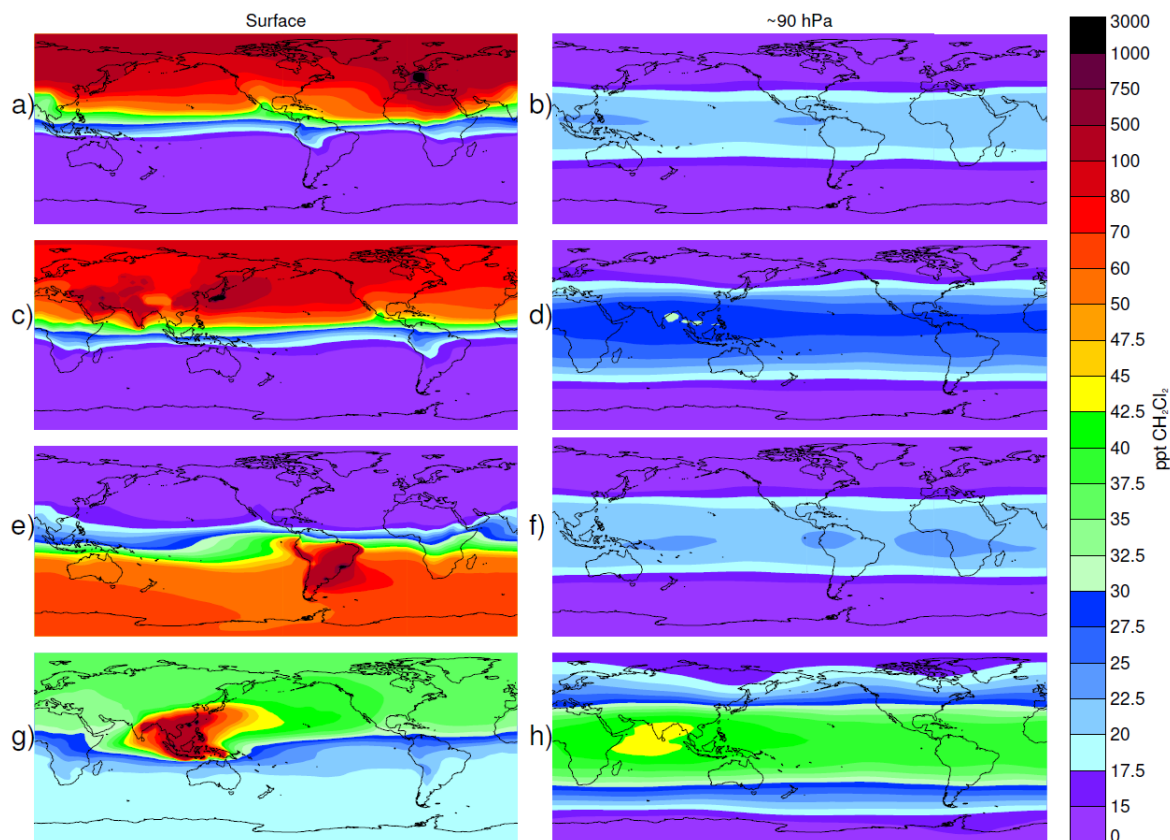


Figure 1. Modelled 5-year annual mean steady-state mixing ratio (ppt) of CH₂Cl₂ at the surface (left) and at 90 hPa (right) based on a 1 Tg/yr emission from (a, b) Europe, (c, d) Temperate Asia, (e, f) Temperate Latin America, and (g, h) Tropical Asia.

Accepted

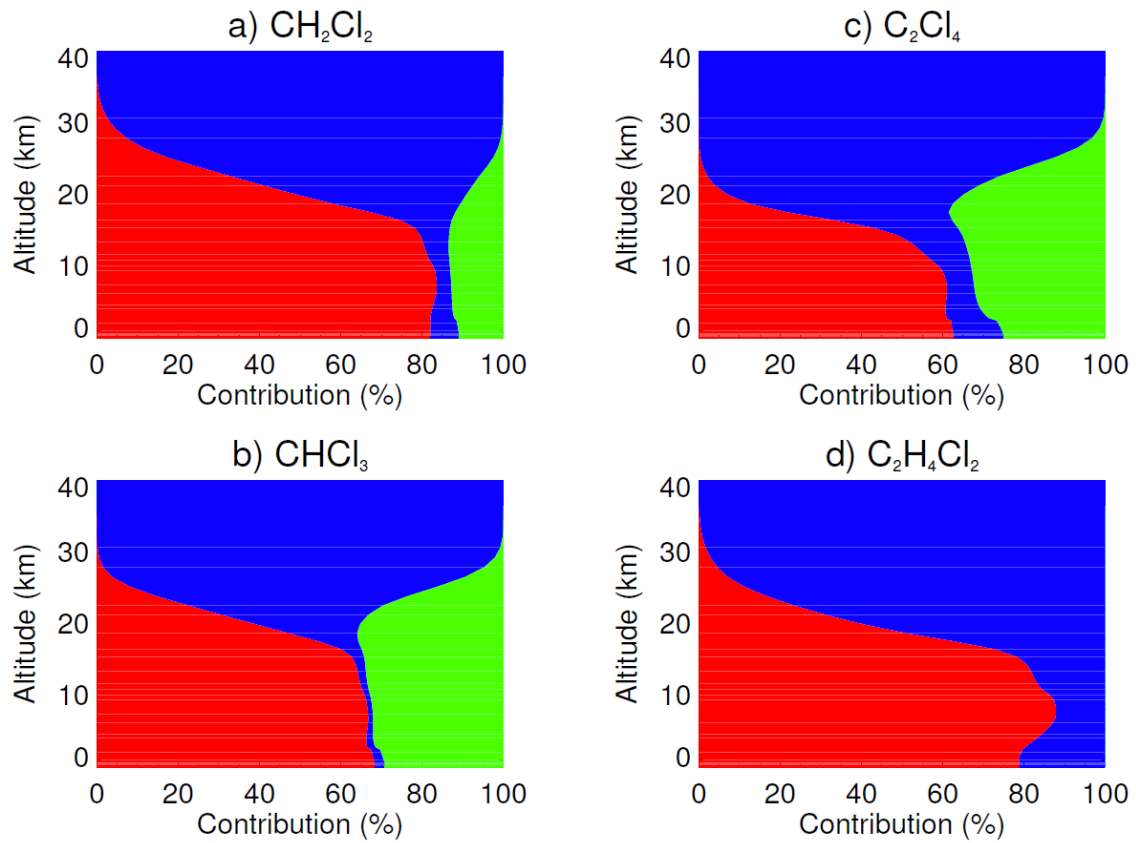


Figure 2. Vertical profile of the contribution (%) of source and product gases to total chlorine from (a) CH_2Cl_2 , (b) CHCl_3 , (c) C_2Cl_4 and (d) $\text{C}_2\text{H}_4\text{Cl}_2$. Contributions are tropical (20°N – 20°S) 5-year means calculated at steady-state following a continuous 1 Tg/yr emission from Europe. Red is the proportion for source gases, blue for Cl_y , and green for COCl_2 (see also **Text S1**).

Accepted

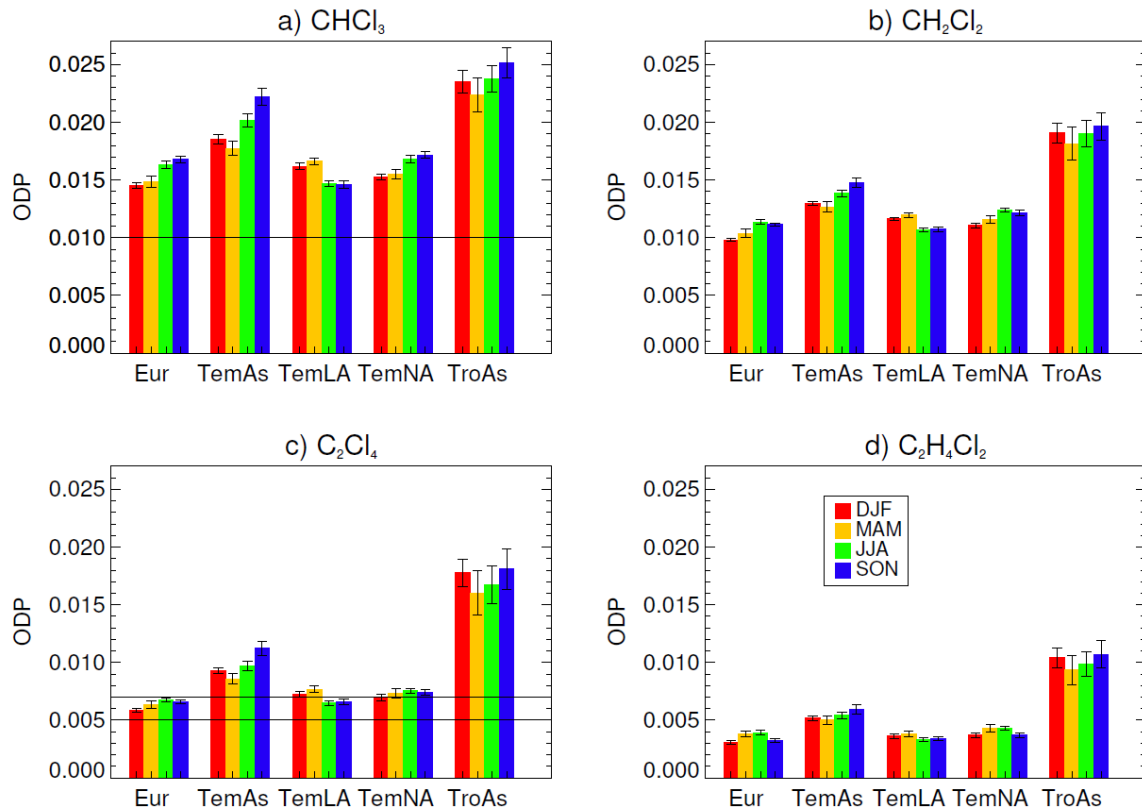


Figure 3. Calculated ODPs for (a) CHCl_3 , (b) CH_2Cl_2 , (c) C_2Cl_4 and (d) $\text{C}_2\text{H}_4\text{Cl}_2$, as a function of emission region and season. Horizontal lines represent literature values: CHCl_3 from Kindler et al. [1995]; C_2Cl_4 from Kindler et al. [1995] (upper) and Wuebbles et al. [2011] (lower). Error bars incorporate uncertainty due to tropospheric and stratospheric interannual variability.

Accepted